

New age fibers: the children of the photonic revolution

R. Haynes^{*a}, J. Bland-Hawthorn^a, M. C. J. Large^b, K. F. Klein^c, G. Nelson^d

^a Anglo-Australian Observatory, PO Box 296, Epping NSW 1710, Australia.

^b OFTC, 206 National Innovation Centre, Eveleigh, New South Wales 1430, Australia.

^c Fachhochschule Giessen-Friedberg, Wilhelm-Leuschner Straße 13, D-61169 Friedberg, Germany.

^d Polymicro Technologies LLC, 18019 North 25th Avenue, Phoenix, Arizona 85023, USA.

ABSTRACT

The Photonics Crystal Fibers (PCFs) also known as “holey” or “micro-structured” fibers herald a new age for optical fibers. The astronomical applications could revolutionize instrument design through: broadband performance combined with excellent UV transmission, extremely large numerical aperture fibers, and aperture transforming fibers improving input coupling/sampling while maintaining a good match between the fiber outputs and the detector pixels. The Photonic Crystal effects can provide unprecedented non-linear effects in materials and when combined with micro-photonics it is expected that a photonic chip will be realized in which optical switching, wavelength dispersion and even wavelength conversion could take place. However, conventional optical fibers are currently the benchmark for many astronomical applications and improvements in the performance of silica fibers are also being made.

In this paper we present a brief review of the current status of photonic crystal fibers with particular focus on the astronomical applications. In addition we present the optical characterization of a new silica/silica broadband fiber that delivers very good transmission from 300nm to 1100nm and beyond.

Keywords: Photonic crystal fibers, micro-structured fibers, holey fibers, silica fibers, broadband fibers, broadband fiber transmission, optical fiber instrumentation, focal ratio degradation.

1. INTRODUCTION

The use of optical fibers to segment and re-format the telescope focal plane has revolutionized both wide and integral field spectroscopy in astronomy and the AAO has developed a large number of instruments based upon optical fibers with such as the wide field multi-object spectroscopy systems 2dF¹, OzPoz², 6dF³, FMOS Echidna⁴ and integral field units (IFUs) such as SPIRAL⁵. Further information on these instruments is also available at the following web site (www.aao.gov.au/AAO/astro/instrum.html). However, with the continued challenges presented by the current 8-10m and future 30-100m ELT class telescopes, instrument builders have to look for more innovative solutions.

Despite the recent slow down in growth of telecommunication industry, the development of optical fibers has come on a considerable way in the past 10 years and there been some significant improvements in the performance of the fibers traditionally used in astronomy. Within the last year, still further improvements of the standard step-index multimode fibers have taken place, the characterization and comparison of the latest broadband fiber from Polymicro technologies is presented in Chapter 3. However, there has also been a revolution in the World of Photonics with the introduction of devices based on Photonic Crystal Structures. These developments may eventually provide astronomy with all sorts of tantalizing possibilities from ultra fast optical computing systems, to fully integrated instrumentation in which the photons never leave a complex photonic structure and are guided, switched, filtered, polarized, dispersed and eventually detected all with a single device attached to a detector. However, this is outside the scope of this paper that concentrates on the recent development of Photonic Crystal Fibers (PCFs) and conventional silica fibers.

2. PHOTONIC CRYSTAL FIBERS (PCFs)

New and exciting prospects for ultra broadband, high numerical aperture and aperture transformation fibers are on the horizon. The recent development of Photonic Crystal Fibers (PCFs) herald a new age for optical fibers and promise all sorts of new fiber phenomena as well as overcoming some of the limitations of conventional optical fibers. This rapidly developing field is being driven by non-astronomical applications, however, the AAO is working closely with groups

* rh@ao.gov.au; phone +61 2 93724815; fax +61 2 93724880; www.aao.gov.au

such as the Optical Fibers Technology Centre (OFTC) to develop promising technologies suitable for future ground and spaced based astronomical instrumentation.

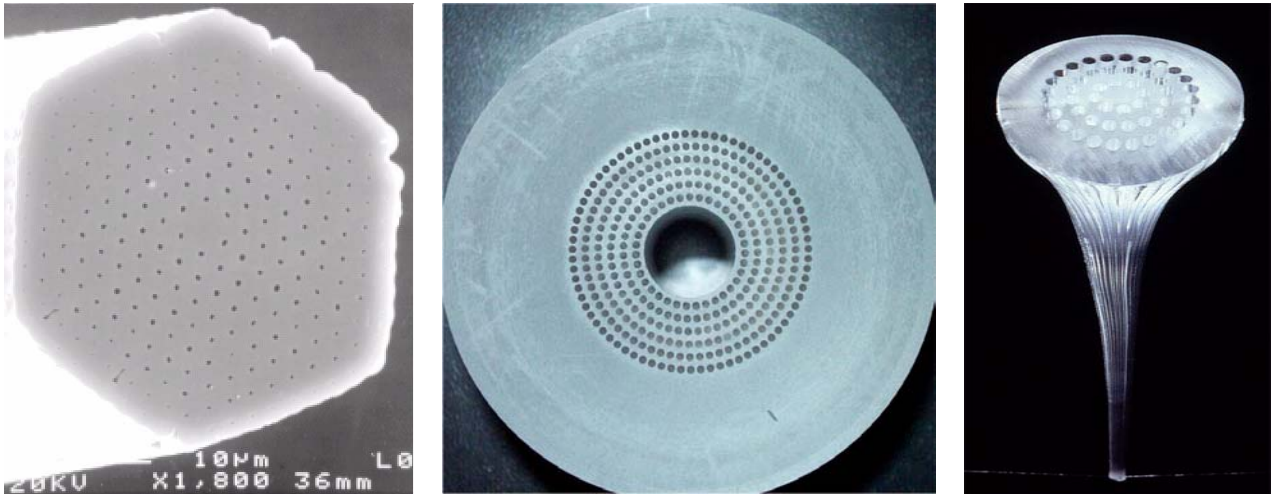


Figure 1: a) Left is an “Endlessly single-mode photonic crystal fiber”⁶ solid core photonic crystal fiber. b) Central is a drilled polymer primary preform manufacture by OFTC (www.oftc.usyd.edu.au). c) Right is the “waste” part of the primary preform (manufactured at OFTC) after the first melt stage in which the preform is drawn into a cane. The cane typically 2-4mm in diameter would then be subjected to a second draw process that produces the polymer photonic crystal fiber.

In the early 1990s it was suggested that a periodic structure or lattice of holes, on the scale of the propagating wavelength, running the length of the cladding could trap light inside a fiber core. Such periodic structures are referred to as photonic crystals and hence the term photonic crystal fibers. By the mid 90s the first working examples of photonic crystal fibers (PCFs), sometimes also known as “holey” or “micro-structured” fibers, were being reported. These solid core PCFs are typically manufactured from silica⁷ (by stacking together rods or capillaries and then drawing the fiber), or from polymer^{8,9} (that can be molded or drilled and then drawn into fiber) and have a solid core of material (in which the light propagates) surrounded by an array of holes that confine the light to within the core. Examples of (a) a solid core PCF and (b & c) polymer preforms are shown in Figure 1.

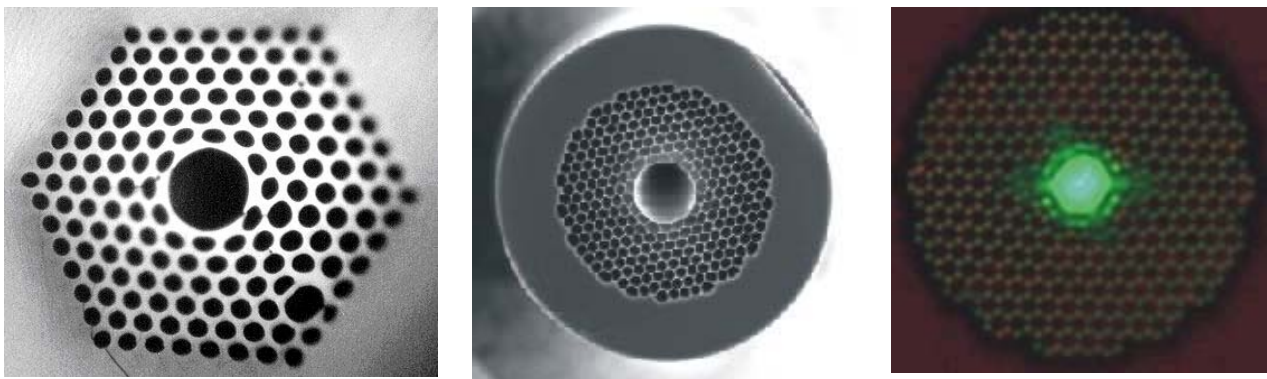


Figure 2 The left hand picture is of an early polymer hollow core fiber manufactured at OFTC. The central picture is a glass hollow core fiber manufacture by Blaze Photonics (www.blazephotonics.com) and the right hand picture shows light that has propagated down the fiber shown in the centre.

Since the first PCF there has been a veritable explosion in the variety of fibers available, matched by the diverse properties and applications of these devices. These photonic crystal structures have opened up a huge, previously inaccessible parameter space in optical fiber technology that is currently limited (primarily) by the difficult fabrication

processes. It is even possible to trap light in a hollow core (typical air) fiber. Such fibers are also referred to as photonic band gap fibers. These work on the same principle as the reflected color of butterfly wings in that periodic structures of similar scale to the wavelength of light exhibit a range of angles and colors in which the incident light is strongly reflected. By wrapping such a structure around a core it is possible to confine light within a hollow fiber core. Examples of hollow core fibers are shown in Figure 2.

2.1. UV, IR power transmission

In photonic band gap fibers the light predominantly propagates in the air within the hollow core and therefore the typical attenuation features associated with the core material are eliminated, with the potential for unprecedented UV and IR performance. This also opens up the possibility of a significant increase in the power that can successfully propagate within the fibers, for example in astronomy this may simplify the optical path and routing for AO laser guide star systems. The power capacity is typically limited by crystal or glass defects within material of the fiber, with hollow core guidance the material effects are massively reduced, being primarily limited to the small amount of energy propagating in the cladding as a result of the evanescent wave. Similarly the attenuation losses typically associated with the core material, such as Rayleigh scattering in the UV and molecular vibration losses in the IR are in principle almost eliminated, although other attenuation features such as confinement loss (leakage of light through the bridges between the holes), surface scattering and irregularities in the structure do contribute to loss. The losses in hollow core fiber have decreased very rapidly in the last 3 years. The most recent low loss figure is 1.7dB/km at 1550nm, reported by Blaze Photonics¹⁰, a seven-fold improvement over the previous record. The real advantage of PCFs for astronomy is likely to be in allowing transmission in areas where material issues have prevented substantial transmission in the past.

Much of the work with PCFs has been concentrated on the near IR telecommunication bands around 1300nm and 1550nm and the PCFs are improving extremely rapidly, though they are still some way from the performance currently available with conventional silica fibers. However, silica fibers start attenuating very heavily beyond $\sim 2\mu\text{m}$, it is hoped that band gap and/or solid PCFs using different core materials will be able to push the wavelength performance into the mid IR and beyond. Conventional fibers are available that can transmit beyond $2\mu\text{m}$; zirconium fluoride from 0.45- $5\mu\text{m}$, chalcogenide fibers from 2- $11\mu\text{m}$ and silver halide fibers from 4- $18\mu\text{m}$, but these have significant absorption features, are often very costly (more than hundred times the cost of similar silica fiber) and are susceptible to moisture and chemical attack. Among other factors the PCFs do not require difficult and time consuming cladding doping processes during manufacturing as the refractive index boundary is provided by the hole structure. During the following year the AAO will be working closely with OFTC on characterizing and developing PCFs with enhance IR performance.

The prospect for UV transmission of hollow core fibers should also be very good in principle, as the Rayleigh scattering is virtually eliminated by propagation in air, however, currently the performance is well below expected levels, and will be much more problematic than for IR transmission. The confinement loss mentioned earlier can be related to the width of the bridges between the holes, as well as the number of rings of holes. For short wavelengths the bridge width required for very low loss is so small that issues of structural stability may be limiting. Surface scattering will also play a more dominant role for shorter wavelengths. However PCFs do in principle have the capacity to improve the blue transmission of fibers, and the field is developing very rapidly. As presented in section 3.1 we already have fibers, which for relatively short lengths, transmit well down to 300nm. These can be used very effectively if the spectrographs can be mounted close to the telescope focal plane. However, for high-resolution ground based UV spectroscopy they would be better remotely mounted from the telescope because of typical size and stability requirements. The goal with PCFs is to have long lengths (50m or more) of optical fibers with high transmission up to the atmospheric cut off ($\sim 300\text{nm}$).

2.2. High Numerical Aperture fibers

With PCFs the effective refractive index of the cladding roughly equates with the average of the air in the holes and that of bulk material in which the holey structure sits. This then allows for very large differences between the core (e.g. silica $n\sim 1.45$) and the cladding refractive index (close to that of air i.e. $n\sim 1$) and hence very large critical reflection angles, allowing very fast beams to propagate down these fibers with a NA as high as 0.9. The critical parameter in producing very high NA fibers is the width of the bridges between the holes, which must be as thin as practically possible¹¹. An example of a section of a high NA PCF is shown in Figure 3.

2.3. PCF Imaging bundles

Another development that has great prospects is imaging PCFs¹¹. An example of a polymer imaging PCF is shown in Figure 4. The primary guiding occurs in the “island” region between the holes, though over short lengths some “anti-guiding” or grazing incidence reflection can be effective within the holes themselves. In this particular the fiber islands are very small compared with the hole structure, however, this island size can be greatly increased to improve the filling factor efficiency of the bundle. In addition if such a structure was coupled using a microlens array, filling factors approaching 100% should be realized, as is typical on convention fiber based IFU⁵.

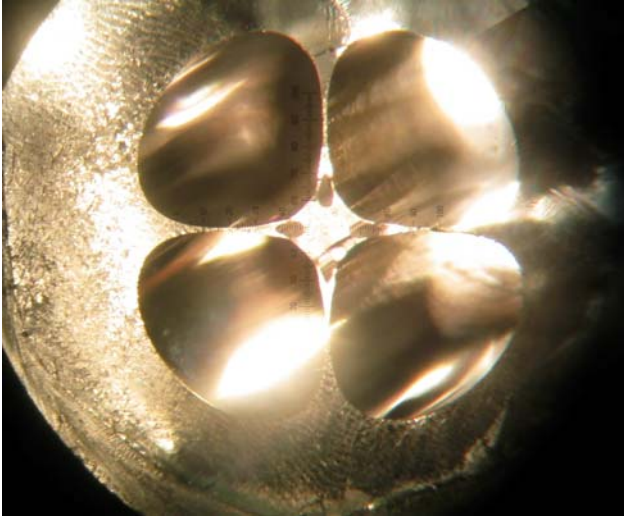


Figure 3: A picture of the intermediate draw stage of a very high NA polymer fiber manufactured by OFTC.

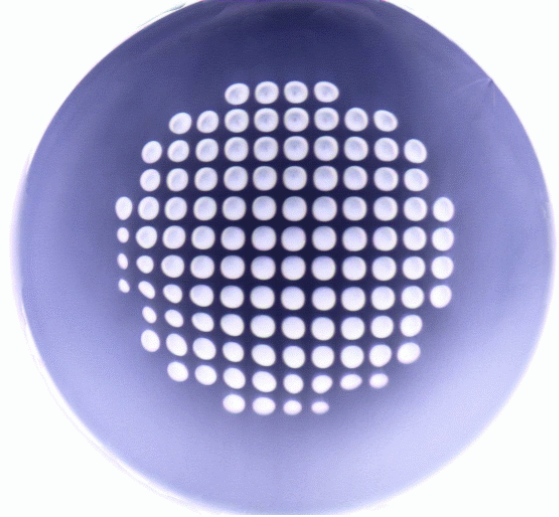


Figure 4: An example of a polymer PCF imaging bundle made at the OFTC. Image courtesy of Martijn van Eijkelenborg.

3. CHARACTERIZATION OF A NEW BROADBAND SILICA FIBER

One of the challenges that typically face designers of fiber based astronomical instrumentation is the requirement for very broadband performance from the UV (possibly down as far as 300nm) through to the IR (1100nm) and beyond. For example, the AAOmega^{18,19} instrument being built at the AAO to replace the 2dF spectrographs has a wavelength range from 370 – 950nm. However, it would be highly desirable to develop a fiber that has a high transmission efficiency all the way down to the atmospheric cut off at ~300nm in order to facilitate high efficiency wide field multi-object spectroscopy (MOS) in the UV using optical fibers. The use of fibers would help eliminate or reduce some of the problems associated with wide field slit based MOS systems such as GMOS²⁰ and image slicer based integral field units (IFUs) such as UIST²¹, by reducing the size and complexity of the optics and in the MOS case improving the efficient use of the detector real estate. Historically fibers that perform well over all of the waveband have not been available, but are now being produced as discussed below. The prospects of UV transmitting PCFs has already been discussed, but efficient transmission below 400nm requires significant development of the current technology for producing PCFs.

3.1. Transmission

The best performing broadband fibers are those with a silica core and doped silica cladding. Historically, these had significant OH absorption bands in the far red and infrared. Chlorine can be used to reduce the OH content to much lower levels, improving the red and IR performance, but the chlorine increases the ultraviolet absorption, which combined with other metal absorption features and the intrinsic structural defects within silica severely impact the blue/UV performance. Instrument designers were given the choice of High OH fibers (sometimes referred to as “wet” fibers) that had significant red and IR absorption bands or Low OH fibers (sometimes referred to as “dry” fibers) that have very high UV absorption primarily dominated by the effects of the chlorine treatment. This enforced a trade off

between either the good blue or good red performance of the final system. The situation significantly improved with the development of the Heraeus STU fiber preforms that provide a better overall broadband performance. However, these fibers were not as effective in the “blue” as the High OH fibers and still have some residual absorption in the “red” around 950nm. Also the manufacturing of the preforms was significantly more expensive than the wet (High OH) and dry (Low OH) preforms and the resultant fiber was typically significantly more expensive. For some fiber systems cost may not be a significant driver, however, for the Gemini telescope WFMOS concept, somewhere in the order of 4800 fibers is envisaged each around 60m in length and around 300km of fiber would be required.

Last year Polymicro Technologies LLC¹³, using improved processing in preform and fiber stage¹⁴, started to offer a new FBP broadband fiber that has excellent transmission performance from below 300nm through to 2000nm (Note: the UV performance of optical fibers below 300nm is discussed in greater detail in papers by Khalilov et al¹⁴ and Ferwana et al¹⁵. The new FBP broadband fiber has comparable performance to the High OH fibers in the “blue”, outperforming the Heraeus STU fiber and is comparable with the Low OH and STU fiber in the “red”).

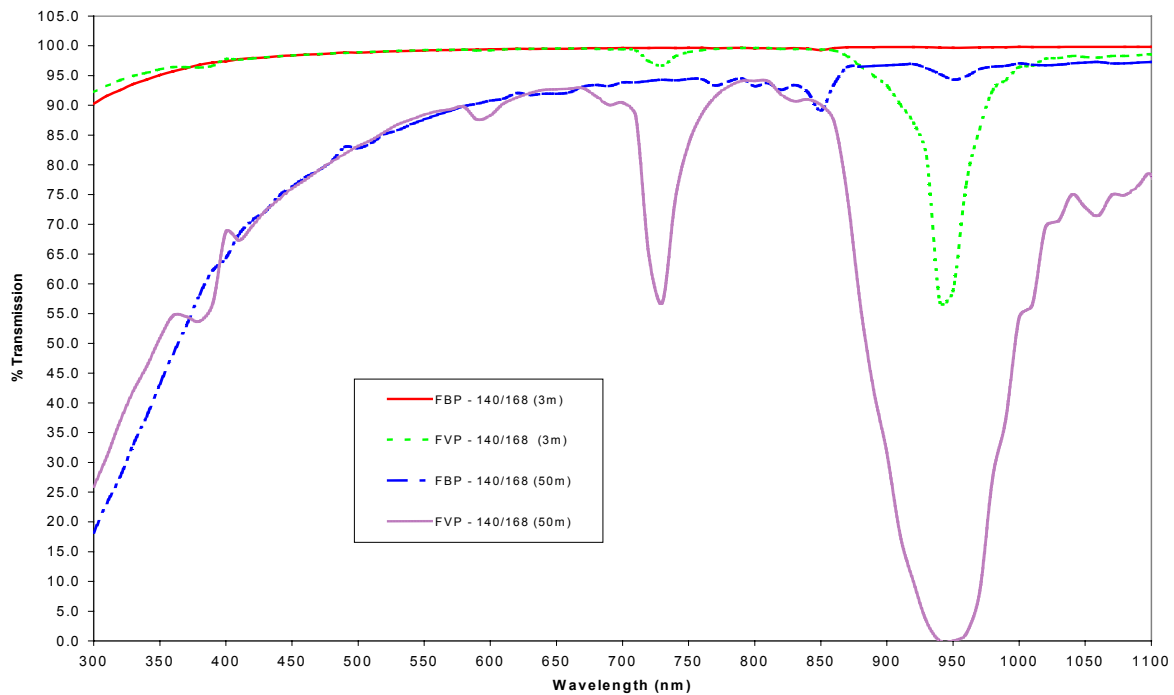


Figure 5: Fiber transmission plot for 3m and 50m lengths of FBP140/168 and FVP140/168 fiber supplied by Polymicro Technologies LLC. The plot shows the internal transmission only and does not include end losses or losses from FRD. Data provided by Polymicro Technologies LLC (www.polymicro.com). Note that the data between 870 and 930nm have been interpolated as data points where not supplied for this region.

Figure 5 shows the transmission data for samples of FBP broadband and High OH (FVP) supplied by Polymicro. The core and cladding diameters in both cases are 140µm and 168µm respectively. Figure 6 shows the transmission data derived from the Polymicro Technologies catalogue¹³ for the typical performance of their Low OH (FIP) and STU (FIPSTU) fibers. The percentage internal transmission is shown for 3m and 50m lengths. It can be seen that the new FBP broadband fiber performs extremely well across the whole “optical” waveband. For a relatively short length (3m) the new FBP broadband fiber transmission at 300nm is over 90% increasing to over 97% by 400nm and continues to improve across the remaining waveband. The STU (FIP STU) fiber has fairly similar transmission characteristics, but is delivering only 83% at 300nm and 96% at 400nm. It should also be noted that the STU fiber is more expensive to produce and can be over twice the price of the FBP broadband fiber. Neither the FVP High OH or FIP Low OH fiber have good broadband transmission over the full waveband, attenuating heavily either in the “blue” (FIP below ~500nm) or the “red” (FVP above ~850nm).

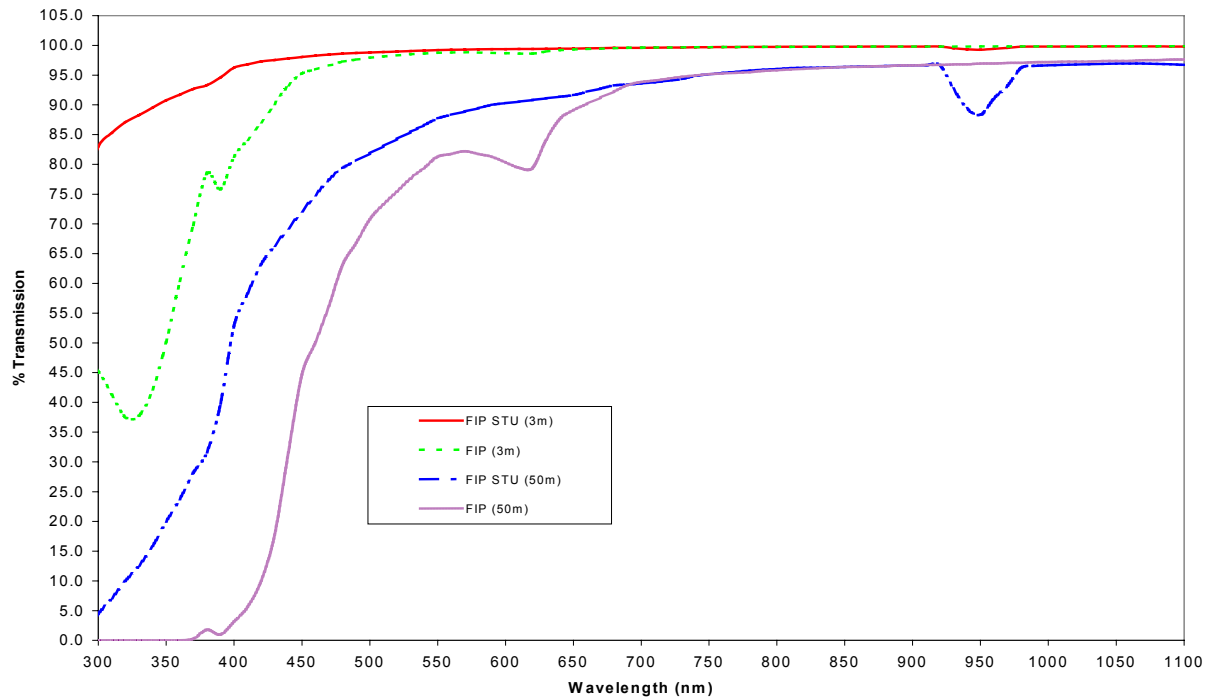


Figure 6: Fiber transmission plot for 3m and 50m length of FIPSTU and FIP fiber supplied by Polymicro Technologies LLC. The plot shows the internal transmission only and does not include end losses or losses from FRD. The data was derived from attenuation plots in the Polymicro Technologies catalogue¹² (www.polymicro.com).

Transmission stability of the FBP fiber has been demonstrated at Polymicro. Recent spectral attenuation plots were identical for two-year-old fibers stored in laboratory environment, thermal cycling tests (-40 deg C to +125 deg C) and thermal ageing tests (100 deg C) yielded no significant attenuation differences.

The performance of this new FBP broadband fiber should benefit future instrumentation and for a relatively small investment it may be possible to significantly enhance the performance of current fiber systems by simply replacing the fiber bundle with this new fiber. It is worth noting that Polymicro may be able to tune the performance of their broadband fiber a little to suit particular requirements, so some optimization may be possible.

3.2. Core/Cladding ratio

When working with optical fibers the rule of thumb is the cladding thickness should be more than ten times the longest propagating wavelength. This is because fibers really behave as circular waveguides and the simply geometric optics model of total internal reflection at the core/cladding boundary is not strictly true. The fibers support electromagnetic waves and part of this (the evanescent wave) extends into the fiber cladding. To allow efficient propagation the cladding must fully support the “tail” of the electromagnetic waves or energy is lost in the buffer (or jacket) surrounding the fiber. The length of the “tail” is dependent on the incidence angle and wavelength of the light, but the fiber should typically be selected to cope with the most extreme red wavelength required.

As an example of core/cladding selection the AAOmega system¹⁸ has a maximum wavelength requirement of 950nm, therefore the cladding thickness should be greater than 9.5µm. Most fibers are supplied with standard core cladding ratios of 1:1.1, 1:1.2 or 1:1.4 and so AAOmega with it 140µm core requirement needs a cladding of greater than 159µm. The nearest suitable core/cladding ratio is 1:1.2 yielding a cladding of 168µm.

3.3. Fiber buffer (Jacket):

The fiber buffer provides a jacket, chemically protecting against environments such as humidity that can cause micro-cracks to develop over time and eventually leading to breakage, as well as some mechanical protection. There are commonly two types buffer materials available, polyimide (a thin very, hard coating) and acrylate (a thicker, softer coating). It is also possible to have a combination of these two with polyimide over-coated with acrylate (“dual buffered”). There are other materials available such a silicone, fluoropolymers and metal coating, but they are not commonly used in astronomy and not available as standard coating from many manufactures. The relative costs of applying an acrylate or a polyimide buffer are about the same. However, the combination coating of polyimide over-coated with acrylate is more expensive as this requires an additional stage in the manufacturing process. The buffer material often used by the AAO for astronomical applications is typically polyimide for a number of reasons, some of which are listed below. However, the choice of buffer is reviewed depending on the specific application.

- Polyimide buffer is a hard low friction material that operates effectively when the fibers move significantly, such as in pulleys within the retractor system of 2dF. Some acrylate coatings can be slightly “sticky”. This can be problematic for retractor systems and when a number of fibers are housed within a single conduit.
- It is necessary to remove an acrylate buffer from the fiber ends if they are to be polished as the soft acrylate allows the fiber to move during the polishing process. This can lead to “rounding off” of the fiber ends with an undesirable optical impact. The removal typically leaves an unprotected region of fiber that is susceptible to chemical and physical damage.
- The coating thickness of polyimide is typically 10-15 μm , where as acrylate is typical 40 μm or greater. In some cases the space and design constraints means smaller fiber external diameters can be an advantage.
- The polyimide buffer appears to offer significantly better mechanical protection to localized stressing effects than the acrylate and “dual buffered” fibers. This is discussed in great detail in the FRD section (3.5).

3.4. Fiber Numerical Aperture

Conventional optical fibers, like the multimode step index silica fibers typically used in astronomy, guide light by the principle of total internal reflection in which light is “confined” within a higher index core surrounded by a lower index cladding. The light incident on the fiber end face can be captured by the fiber and propagate along the core. Shortly, it will strike the core/cladding interface and provided the strike angle is less than the critical angle (θ_{max}) the light is completely reflected. The number of reflections will depend on the length, core size, angle of incidence and the wavelength of the light, and may occur many thousands of times along the fibers length. If the angle of incidence is greater than the critical angle some light will be lost at each reflection and light will therefore not be efficiently guided. The angle at which the transition between total and partial internal reflection takes place is the numerical aperture (NA) of the fiber and is set by the refractive index difference between the core and cladding material, as defined below.

$$\text{NA} = \text{Sin } \theta_{\text{max}} = \sqrt{n_{\text{core}}^2 - n_{\text{cladding}}^2} = \frac{1}{2 \times F_{\text{number}}}$$

Where n_{core} is the refractive index of the fiber core, n_{cladding} is the refractive index of the cladding, θ_{max} is the maximum angle to the fiber axis at which a meridional ray entering the fiber will be efficiently guided. For astronomical application the NA is an important parameter as it sets the minimum F_{number} at which the fiber can be fed. Multimode step index silica fibers typically have an NA of around 0.22 ($\sim f/2.3$), however, they can be as high as 0.37 in silica/hard polymer clad optical fibers¹³ or even 0.66 in Silica/Teflon AF clad optical fibers¹³. The NA performance of the Polymicro FB_ broadband fiber is nominally specified as 0.22 and characterization of this parameter is given in a complimentary paper by Ferwana et al¹⁵.

3.5. Focal Ratio Degradation (FRD)

For those involved in the design optical fiber instrumentation for astronomy, focal ratio degradation (FRD) will be a very familiar parameter. For those less familiar, FRD is a characteristic of optical fibers in which the input beam cone angle is “blurred”, or more specifically widened as a result of propagation along the fiber. An input beam cone angle is typically increased from some angle θ to approximately $\theta + 1/2\Delta\theta$. This $\Delta\theta$ “blurring”, that scatters light both “into” the beam as well as “out of” the beam, is not constant and varies considerably with input angle. A consequence of the FRD

is a degradation of the Etendue (increase in $A\Omega$ product) within the optical system. Laboratory testing of the extent and susceptibility of various fiber types to FRD are discussed below. The tests were primarily designed to determine the fiber characteristics for the AAOmega project¹⁸, however, they were made as generic as possible within the time and budget constraints. The tests were carried out using a laser beam incident on the fiber input face at various different input angles and the amount of angular “smearing” (FRD) for that input angle was determined. This was quantified in terms of the FWHM of the radial profile for the corresponding fiber far-field output ring. The details of the FRD test procedure is described more thoroughly in Ferwana et al¹⁵. This technique was chosen for fiber comparison studies, as it is very sensitive to small differences in fiber performance.

The first test was the study of FRD as a function of input angle for a 1m long fiber of different core types and buffer materials. For all fibers, except the STU, the core and cladding diameters were 140 μ m and 168 μ m respectively.

Input Angle	0°	2°	4°	6°	8°	11°	14°
Numerical aperture	0	0.03	0.07	0.10	0.14	0.19	0.24
Effective f/ratio	f/∞	f/14.3	f/7.2	f/4.8	f/3.6	f/2.6	f/2.1
1 FBP 140/168	1.7	3.4	2.2	1.3	1.1	0.9	0.9
2 FVP 140/168	1.8	2.9	3.2	1.2	1.0	0.8	0.8
3 FBA 140/168	1.1	4.3	2.7	1.2	1.0	0.8	0.8
4 FVA 140/168	1.9	3.7	3.5	1.4	0.9	0.9	0.9
5 FVP 140/168 (2dF)	2.2	2.5	1.5	1.3	1.1	1.0	1.4
6 FBPA 140/168	1.6	1.7	2.5	1.4	0.9	0.9	0.7
7 FIPSTU 100/110	2.2	2.9	2.3	2.1	2.1	1.8	-
8 FIPASTU 100/110	3.0	4.0	4.9	2.9	2.8	2.5	-

Table 1: FWHM (in degrees) of the radial profiles for the far field illumination pattern over a range of fiber types and different input angles for a fiber 1m in length. The FV_ designation is High OH fiber, the FB_ is Broadband fiber, the FI_STU is fiber, and the A and P designation correspond to acrylate and polyimide buffer. The 2dF fiber is an FVP and an identical specification to the FVP fiber, but supplied around 1996. Note, there are input angle zero point errors of up to +/- 0.5 degrees. In all cases the fiber was cleaved and there may be cleave angle errors up to 1°, except for fiber 5 that was terminated with a stainless steel tube and polished.

The results for the STU fiber are from a 100 μ m core fiber and unpublished work at the AAO has observed that FRD typically increase slightly with reduced fiber core size, so poor performance might be expected. From Table 1 it can be seen that the intrinsic FRD performance (un-stressed) for most of the different fiber types is small and at 8° varies between a FWHM of 0.9° and 1.1° within the experimental errors of the order $\pm 0.1^\circ$, the exceptions are the STU fibers. An experiment carried out on different lengths of the FBP140/168 fiber showed little change in FRD performance between 0.5m and 36m degrading the FWHM of the profile from 1.0° to 1.2°. This small length dependence is very difficult to explain using geometric optics arguments based on inhomogeneity and defects perturbing or scattering the beam, as the FRD would be expected to scale with length. However, from a modal perspective, in which an input beam excites a number of modes in the fiber, the weak length dependence is understandable and is discussed later in section 3.6. It can be seen in Figure 7 that for small input angles (4° and less) it is difficult to resolve a clear ring produced by the fiber and providing a quantification of the radial profile can be misleading, however, it is clear that the amount of “blurring” or FRD is much higher at small input angles than larger input angles. Astronomers have known this phenomenon for many years. It is generally agreed that, where possible, you should feed fibers with beams faster than f/5 ($\sim 6^\circ$) in order to reduce the FRD losses in the system. This can also be seen in Table 1 where the FWHM of the radial profiles is in some cases more than half that at f/7.2 (4°).

As an example the 2dF system for the Anglo Australian Telescope feeds the fibers at $\sim f/3.4$ and the new AAOmega spectrograph will be fed by 36m of the Polymicro FBP 140/168 fiber. Approximating the fiber FRD profile to that of a Gaussian with a value of 1.2° FWHM (that of a 36m length of FBP fiber). The FRD would degrade the f/3.4 input beam such that 95% of the encircled energy would be confined within an f/3.4 beam and 99% within an f/3.1 beam. Note these results do not account for central obstruction generated by the hole in the primary mirror (\sim equivalent of f/8) that shifts the values to 95% within f/3.3 and 99% within f/3.0 respectively and are almost identical to the results for a 1m length. This relatively small length dependence is also observed by Ferwana et al¹⁵.

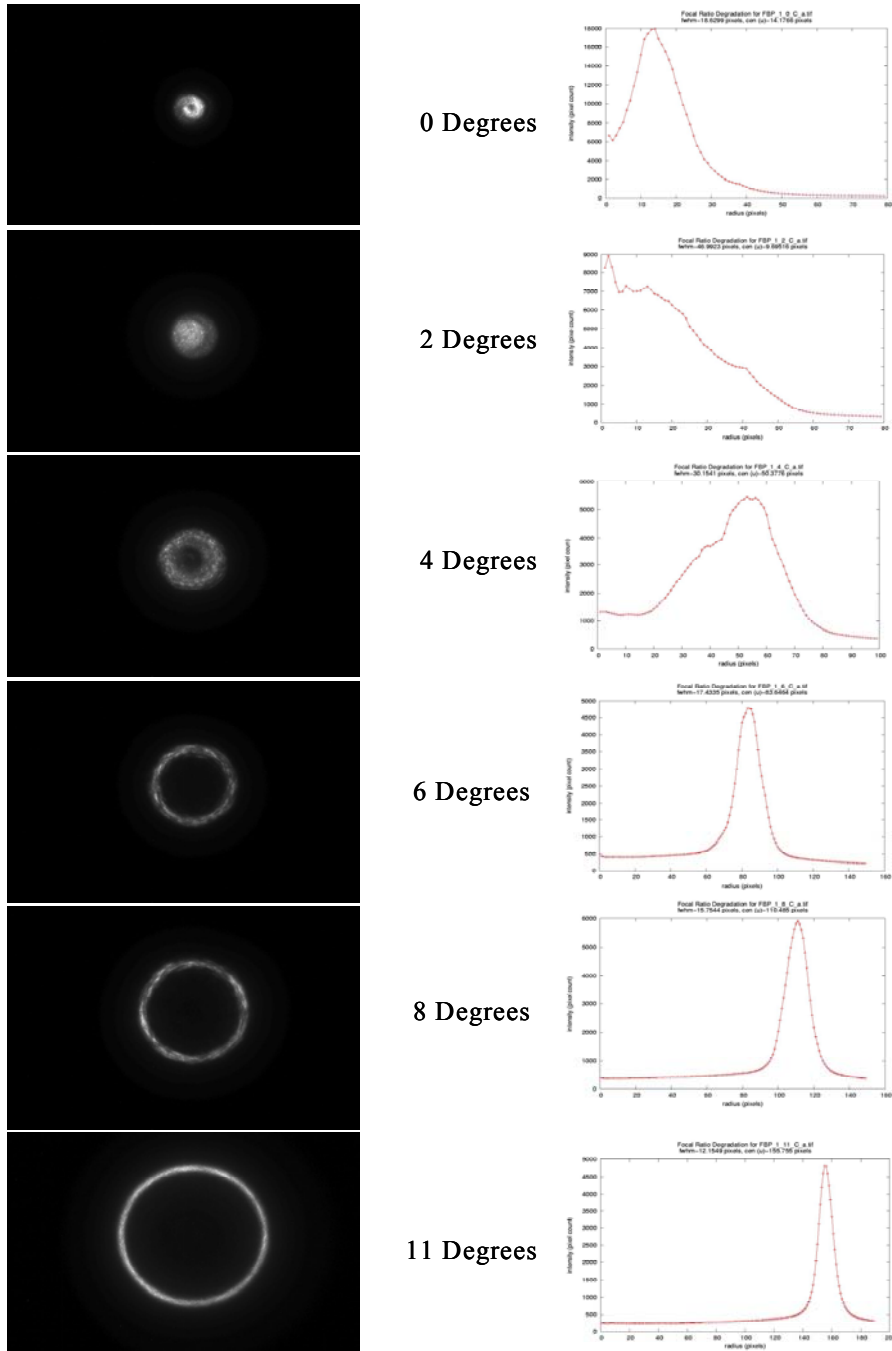


Figure 7: The left hand pictures are the far field light distributions from polyimide coated broadband fiber (FBP140168198) with a core size of $140\mu\text{m}$. The right hand pictures are the radial profile plots corresponding to the left hand images. Note the horizontal scales on the radial plots are 80, 80, 100, 160, 160, 200 and 250 pixels respectively.

To simulate bends within at typical fiber run the FRD test results from an experiment to quantify the impact of bending the fibers are presented in Table 2. The fibers are bent $\sim 180^\circ$ around different diameter cylinders. For the AAOmega fiber system the most extreme bends are in the fiber retractor modules and fiber slit assembly. We have set minimum bend diameter of 60mm (for 170 μ m cladding diameter fiber), this is well above the critical bend radius (~ 8 mm) at which the fiber may fail, as relatively large diameter bends can have an impact on FRD as is observed. The minimum usable bend diameter will be strongly dependent on the fiber diameter. From Table 2 it appears that susceptibility of fibers to bending induced FRD is slightly greater in the broadband fiber (FB_) fiber than the High OH fiber (FV_), but the buffer (_A or _P) appears to make little systematic impact.

Fiber Type	Bend diameter (mm)				
	58	47	33	25	13
1 FBP 140/168	1.0	1.1	1.5	2.7	2.7
2 FVP 140/168	0.9	1.1	1.3	2.1	2.3
3 FBA 140/168	1.0	1.1	1.9	2.7	2.7
4 FVA 140/168	1.0	1.1	1.1	1.7	1.9
5 FVP 140/168 (2dF)	1.2	1.1	1.7	2.4	3.0

Table 2: FWHM (in degrees) of the FRD broadening for 1m lengths of different fiber types bent $\sim 180^\circ$ around different diameter and an input angle of 8° (NA 0.14, $f/3.6$). FV_ designation is High OH Fiber, the FB_ is broadband fiber, and the A_ and P_ designations correspond to acrylate and polyimide buffer. The 2dF fiber is an FVP and an identical specification to the FVP fiber, but supplied around 1996.

Historically, some fiber based astronomical instruments have some not performed as well expected. In some cases this was later traced to poor FRD performance as a result of external stressing of the fiber at points along the fiber run. This external stressing of the fiber can have a very dramatic effect as is shown and remains a critical consideration in the design of fiber bundles. A stress test was set up in which the fiber was placed on the hard flat surface and various weights were placed on the fiber via two small contact points. This is to simulate clamping and gluing points in the fiber run. The susceptibility of the fiber to point stress inducted FRD is shown in Table 3. It can be clearly seen that the polyimide buffer provides significantly better protection than either the acrylate or combination buffer and there is no systematic difference between the choices of fiber core material. It is also seen that the impact of external stressing on the fiber FRD properties can be huge and dominating the fiber performance. The FRD was so bad for the purely acrylate buffered fibers that it was not possible to determine a meaningful FWHM value.

Fiber Type	Point contact load on the fibers				
	0g	100g	200g	300g	1000g
1 FBP 140/168	1.0	1.6	1.8	1.9	3.2
2 FVP 140/168	1.0	1.3	1.7	2.1	3.6
3 FBA 140/168	1.0	2.0	4.0	4.7	-
4 FVA 140/168	1.0	2.3	4.7	5.7	-
5 FVP 140/168 (2dF)	1.1	1.7	2.1	2.4	4.5
6 FBPA 140/168	1.0	2.1	3.1	3.5	6.1
7 FVPA 140/168	1.0	2.3	3.0	3.5	9.6

Table 3 FWHM (in degrees) of the FRD broadening under different point load conditions for 1m lengths of different fiber types. An input angle of 8° (NA 0.14, $f/3.6$) was used. FV designation is High OH fiber, the FB is broadband fiber, and the A and P designation correspond to acrylate and polyimide buffer. The 2dF fiber is an FVP and an identical specification to the FVP fiber, but supplied around 1996.

3.6. FRD in terms of waveguide modes in multimode fibers:

It is not within the scope of this paper to discuss the many aspects of the propagation of modes within fibers and there are numerous texts available that discuss this in detail, however, there are some of properties important to astronomical applications that can only be explained adequately using a modal approach.

In a simple geometric optics approach light can propagate within the fiber at any angle relative to the fiber axis that does not exceed the critical angle reflection criteria. Solving Maxwell's equations for an optical fiber yields a series of discrete solutions called "modes", and the number of modes that are guided is limited. Modes only propagate efficiently if the wavefront for that mode remains in phase at each successive reflection, i.e. an integer number of wavelengths between successive reflection points. It should be evident that the modes supported within the fiber will strongly depend on the refractive index profile, the wavelength of the light, and the fiber cross sectional dimensions and there are not just meridional, but also oblique and spiral mode "paths" within the fiber. For the multimode fibers used in astronomy, with core sizes 100µm or greater and operating at optical or near IR wavelengths, can typically support many hundreds of modes.

A very useful fiber parameter that summaries many important characteristics is the "V" parameter defined below, where d is core diameter, λ is wavelength n is refractive index, NA is numerical aperture and N is number of modes.

$$V = \frac{\pi d}{\lambda} \sqrt{n_{core}^2 - n_{cladding}^2} = \frac{\pi d}{\lambda} NA \quad , \text{ and for a multi-mode step index fiber } N = \frac{V^2}{2}$$

Note: the second formula counts, in cases where the states are degenerate, both orthogonal polarizations of the one mode as separate modes.

In an idealized fiber (no geometric irregularity, a homogenous core material and refractive index and no micro-bends) there should be little power transfers. Those modes that are initially excited will be strongly dependent on the input illumination distribution. Each mode will have associated angular distribution in geometric terms, and the lower the order of the mode the greater the width of distribution. Furthermore, light launched at small angles relative to the fiber axis will preferentially excite low order modes and higher order modes are excited by large incident angles. Therefore launching a laser beam (with negligible angular distribution) into a fiber will excite modes that have a finite angular distribution that will be dependent on input angle. The result is a decreasing FRD with an increasing input angle. In an idealized fiber the FRD should be independent of the fiber length, however, material irregularities, variations in fiber geometry as well as bending and microbending, perturb the modes and modal coupling occurs that transfers energy to different "angles". However, the level of modal crosstalk will depend strongly on the amount of perturbation. In a well-manufactured fiber, which is not subjected to significant external stress, the perturbation may be very small. Therefore it is reasonable to expect that the intrinsic fiber FRD will exhibit only a weak dependency on fiber length as observed.

CONCLUSIONS

Photonic crystal fibers represent a new paradigm with far reaching possibilities for astronomy. This recent development is growing and changing rapidly and the AAO is working closely with partners within the field in order to realize the potential this technology has for revolutionizing fiber-based instrumentation. There are a number of areas highlighted in the paper, such as imaging bundles, IR and high power transmission that appear highly promising in the short term, others such as UV transmission and strong non linear properties that are likely to take longer to develop to a level suitable for mainstream astronomical applications. Conventional fiber technology have also developed significantly and the new broadband fiber now available from Polymicro has excellent transmission from ~300nm to ~2000nm along with very good FRD performance. This should be a significant benefit to UV and broadband fiber astronomy. However, as test results demonstrate, fibers are particularly susceptible to their mechanical environment requiring careful system design for fiber base instrumentation.

ACKNOWLEDGMENTS

The authors thank their colleagues Leon Poladian, Wayne Padden, Nader Issa, Martijn van Eijkelenborg and Simon Fleming (OFTC) for productive discussions, Dionne James (AAO) for assistance in with laboratory testing and data reduction, Rick Timmerman (Polymicro Technologies) for optical fiber testing, and PPARC for funding the research through the "Astrophotonics" innovative technology scheme.

REFERENCES

1. J. Lewis, et al, "The Anglo-Australian Observatory 2dF facility", *MNRAS*, **Vol. 333** pp. 279-299, 2002.
2. P. R. Gillingham, D. Popovic, T. J. Farrell, L. G. Waller, "The performance of OzPoz, a multi-fiber positioner on the VLT", *Proceedings of the SPIE*, **Vol. 4841**, pp 1170-1179, 2003.
3. W. Saunders, et al, "6dF sees the light!", *Anglo-Australian Observatory - Newsletter (ISSN 0728-5833)*, **No. 97**, p. 14 – 17, 2001.
4. P. R. Gillingham & A. M. Moore, et al, "The Fiber Multi-object Spectrograph (FMOS) Project: the Anglo-Australian Observatory role", *Proceedings of the SPIE*, **Volume 4841**, pp. 985-996, 2003.
5. D. Lee and K. Taylor, "Fiber developments at the Anglo-Australian Observatory for SPIRAL and AUSTRALIS", *Proceeding of the SPIE*, **Vol. 4008**, p. 268-276, 2000.
6. T. A. Birks, J. C. Knight, and P. St. J. Russell, "Endlessly single-mode photonic crystal fiber", *Opt. Lett.* **22 (13)** 961-963, 1997.
7. Bjarklev A., Broeng J., Bjarklev A. S., *Photonics Crystal Fibres*, Kluwer Academic Publishes, Sept 2003.
8. M. A. van Eijkelenborg, et al, "Recent progress in microstructured polymer optical fibre fabrication and characterization", *Optical Fiber Technology*, **Vol. 9**, No 4 pp. 199-209, 2003.
9. G. Barton, M. A. van Eijkelenborg, G. Henry, M. C. J. Large and J. Zagari, "Fabrication of microstructured polymer optical fibres", *Optical Fiber Technology*, 2004.
10. B. J. Mangan, et al, "Low loss (1.7 dB/km) hollow core photonic bandgap fiber", Optical Society of America, 2004.
11. N. A. Issa, "High numerical aperture in multimode microstructured optical fibers", *submitted to Applied Optics*, 2004.
12. M. A. van Eijkelenborg, "Imaging with microstructured polymer fiber", *Opt. Express* **12 (2)**, pp 342-346, 2004.
13. Polymicro Technologies LLC, *The Book*, available from Polymicro technologies LLC.
14. Valery Kh.Khalilov, Karl-Friedrich Klein, Gary Nelson, "Low-OH all-silica fiber with broadband transparency and radiation resistance in the UV-region", *Proceedings of the SPIE*, **Vol. 5317**, paper 5317-9, 2004.
15. Saleh Ferwana, Hanns-Simon Eckhardt, Thorsten Simon, Karl-Friedrich Klein, Roger Haynes, Valery Kh.Khalilov, Gary Nelson, "All-silica fiber with low or medium OH-content for broadband applications in astronomy", *Proceedings of the SPIE*, **5494-76**, 2004.
16. G. Lu, G. F. Schotz, J. Vydra, D. Fabricant, "Optical Fiber for UV-IR Broadband Spectroscopy", *Proceedings of the SPIE*, **Vol. 3355**, 884-891, March 1998.
17. Maryanne C. J. Large, et al, "Microstructured Polymer Optical Fibers: Progress and Promise", *Proceedings of the SPIE*, **Vol. 4616**, Paper 33, Jan 2002.
18. W. Saunders, T. J. Bridges, P. Gillingham, R. Haynes, G. A. Smith, S. Croom, D. Jones and C. Boshuizen "AAOmega: a scientific and optical overview", *Proceedings of the SPIE*, **5492-146**, 2004.
19. G. Smith, W. Saunders, T. Bridges, V. Churilov, A. Lankshear, J. Dawson, D. Correl, L. Waller, R. Haynes, G. Frost "AAOmega: a multipurpose fiber-fed spectrograph for the AAT", *Proceedings of the SPIE*, **5492-148**, 2004.
20. R. G. Murowinski et al. "Gemini-north multiobject spectrograph optical performance", *Proceedings of the SPIE*, **Vol. 4841**, pp 1440-1451, 2003.
21. S. P. Todd, M. Wells, S. K Ramsay-Howat, P. R. Hastings "Cryogenic image slicing IFU for UKIRT: manufacture, alignment, laboratory testing, and data reduction", *Proceedings of the SPIE*, **Volume 4842**, pp. 151-161, 2003.
22. Philip Russell, "Photonic Crystal Fibers", *Science*, **Volume 299**, 358-362, Jan 2003.
23. H. J. R. Dutton, "Understanding Optical Communications", The ITSO Networking Series, Prentice-Hall PTR, 1998.
24. Editor S. C. Barden, *Fiber optics in Astronomy*, PASP conference series, **Vol. 3**, 1988.
25. Editor P. M. Gray, *Fiber optics in Astronomy II*, PASP conference series, **Vol. 37**, 1993.
26. Editors S. Arribas, E. Mediavilla and F. Watson *Fiber optics in Astronomy III*, PASP conference series, **Vol. 152**, 1998.
27. Editor S. C. Barden, *Fiber Optics in Astronomical Applications*, SPIE, **Vol. 2476**, 1995.